ANALYSIS OF THE BEAVRS BENCHMARK USING CASMO5/SIMULATE5 WITH JENDL-4.0 AND ENDF/B-VII.1

FUJITA Tatsuya * and SAKAI Tomohiro

Regulatory Standard and Research Department,
Secretariat of Nuclear Regulation Authority (S/NRA/R)
1-9-9, Roppongi, Minato-ku, Tokyo, 106-8450, Japan

tatsuya_fujita@nsr.go.jp, tomohiro_sakai@nsr.go.jp

ABSTRACT

The BEAVRS benchmark was analyzed using the CASMO5/SIMULATE5 in order to compare the measurement data and the calculation results based on the JENDL-4.0 and ENDF/B-VII.1 and investigate the difference between those calculation results. For the hot zero power (HZP) physics test, the calculation results showed good agreement with the measurement data for both of cycles 1 and 2. For cycle 1, the calculation results of the isothermal temperature coefficient (ITC) differed from the measurement data by approximately 1 pcm/°F, and the same tendency has been reported in previous studies. For the cycle operation, the calculation results of the boron letdown agreed well with the measurement data. On the other hand, some calculation results of the axial detector signals had a large difference from the measurement data, which is supposedly attributed to the discrepancy of the axial offset (AO) caused by the authors' approximation for the control rod and shutdown bank positions. In terms of the comparison between the JENDL-4.0 and ENDF/B-VII.1, although approximately 15 ppm difference of the boron letdown in the cycle operation was observed, no significant difference was seen for other core parameters, thus, the influence of the two nuclear data library was small on the present results.

KEYWORDS: BEAVRS Benchmark, CASMO5, SIMULATE5, JENDL-4.0, ENDF/B-VII.1

1. INTRODUCTION

The CASMO5/SIMULATE5 [1,2], which is developed by Studsvik Scandpower, Inc., has been utilized in the Regulatory Standard and Research Department, the Secretariat of Nuclear Regulation Authority (S/NRA/R) in order to simulate the core characteristics of a light-water reactor (LWR) during normal operation and to calculate several important parameters, including the reactivity and peaking factor of a core.

The Massachusetts Institute of Technology (MIT) computational reactor physics group proposed the Benchmark for Evaluation and Validation of Reactor Simulations (BEAVRS) [3]. The BEAVRS benchmark is a new multi-cycle full-core pressurized water reactor (PWR) depletion benchmark based on two operational cycles of a commercial nuclear power plant. It provides a detailed description of fuel assemblies, core loading patterns, in-core fission detector signal data, and other information. In recent

* Corresponding Author

years, many papers concerning the BEAVRS benchmark have been published, in which both of the Monte-Carlo and deterministic methods are applied to simulate the hot zero power (HZP) physics test and cycle operation [4-12]. In addition to such nominal calculations, the uncertainty has also been analyzed based on the random sampling method [10,12].

To compare the LWR core analysis results based on different nuclear data libraries and investigate the difference between those, the authors focused on the BEAVRS benchmark and simulated it by the CASMO5/SIMULATE5 using the JENDL-4.0 and ENDF/B-VII.1. In the present study, the HZP physics test and cycle operation of cycles 1 and 2 were analyzed. For the HZP physics test, the critical boron concentration (CBC), control rod bank worth (CRBW), and isothermal temperature coefficient (ITC) were estimated, and for the cycle operation, the CBC and radial/axial detector signal distributions are estimated in this paper.

2. CALCULATION MODEL

In this study, the CASMO5 calculations were performed with the JENDL-4.0 and ENDF/B-VII.1 [13-15] based on the method of characteristics in order to generate assembly-homogenized cross sections, which were used in the SIMULATE5. Each fuel assembly in the BEAVRS benchmark is a 17×17 lattice containing 1.6 to 3.4wt% UO_2 fuel rods, guide tubes, and an instrument tube. Some fuel assemblies also contain burnable absorber rods of the borosilicate glass. To generate assembly-homogenized cross sections of the fuel assembly section, lattice physics calculations in the single assembly geometry with the mirror boundary condition were performed in 95 energy groups. For the reflector section, the top, bottom, and radial reflectors were modeled as a stack of slabs considering several core components (e.g., support plates, a core barrel, and neutron shield panels). The CASMO5 calculations were performed in 95 energy groups with the black (the zero neutron flux) boundary condition for the section outside of the reflector and the mirror boundary condition for the neighboring fuel section. The SIMULATE5 calculations were p erformed in four energy groups based on the simplified P3 theory.

The fuel loading pattern of the BEAVRS core in cycles 1 and 2 is shown in Figure 1 [3]. In the cycle 1 core, 1.6wt%, 2.4wt%, and 3.1wt% fresh UO_2 fuel assemblies are loaded. Some of those used during the cycle 1 operation, and 3.2wt% and 3.4wt% fresh UO_2 fuel assemblies are loaded in the cycle 2 core.

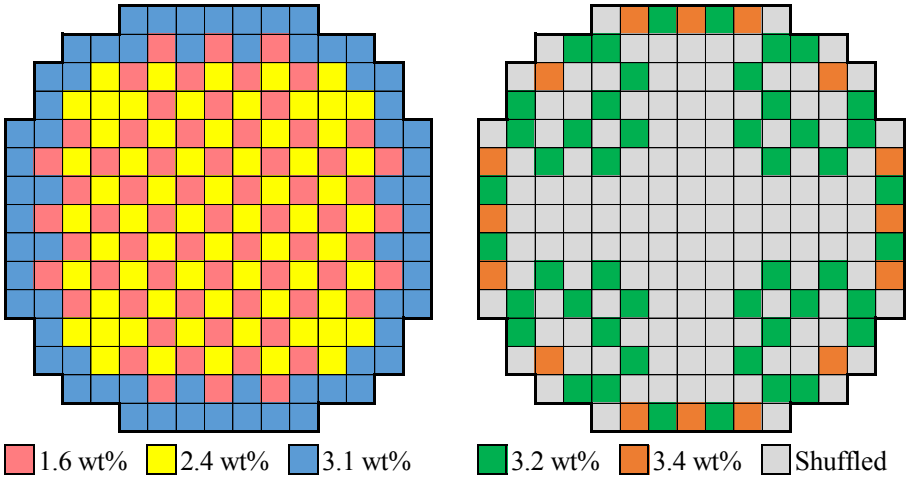

Figure 1. Fuel Loading Pattern (Left: Cycle 1, Right: Cycle 2).

In the BEAVRS core, there are four control rod banks of A, B, C, and D, and five shutdown banks of S_A, S_B, S_C, S_D, and S_E. The positions of the control rod and shutdown banks are illustrated in Figure 2.

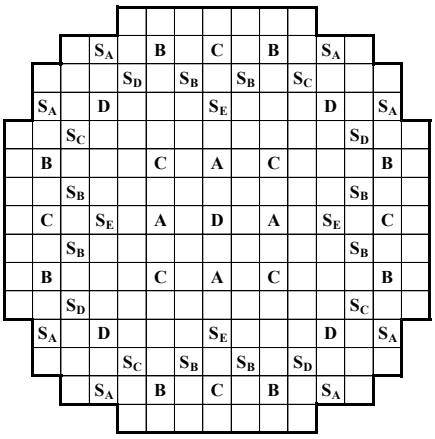

Figure 2. Control Rod and Shutdown Banks.

For the HZP physics test calculation, the core condition is provided in Table I [3]. Although this core condition has been described for cycle 1 in reference [3], the authors assumed that the core conditions in cycle 2 were the same as those presented in Table I since details on the condition for cycle 2 are not provided in reference [3]. The measurement data of the CBC, CRBW, and ITC are provided for the HZP physics test, thus, the measurement data and calculation results are compared later.

Table I. Core Condition of HZP Physics Test.

Parameter	Value
Core Power	25 MWth (approximately 0.73% of full power)
Core Flow Rate	61.5×10^6 kg/h (100% of full flow rate)
Inlet Coolant Temperature	566 K (560 °F)

For the cycle operation calculation, the measurement data of the core power, boron letdown, and radial/axial ^{235}U fission chamber detector signals are provided. The cycle operation diagrams of the calendar days from the beginning of cycle (BOC) are shown in Figures 3 and 4 [3].

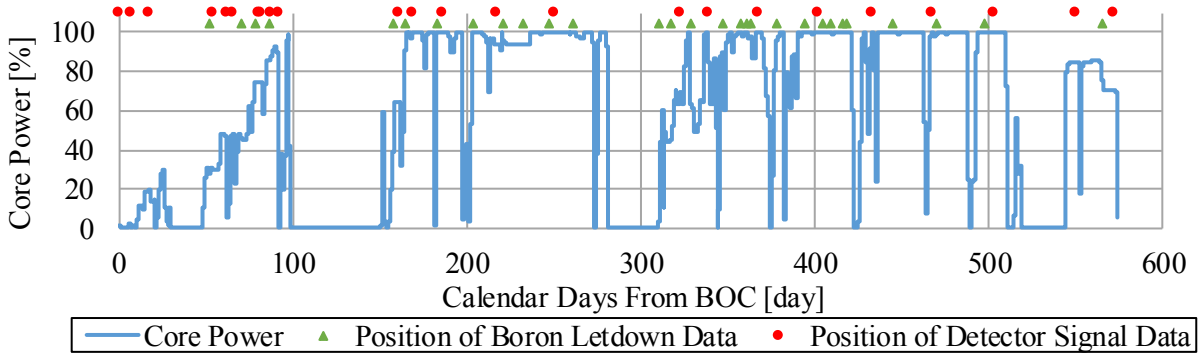

Figure 3. Cycle 1 Operation Diagram.

The core condition and control rod and shutdown banks positions are not described in reference [3]. Thus, the authors assumed that the core power was 3411 MWth (100% of full power), the core flow rate was 61.5×10^6 kg/h (100% of full flow rate), the inlet coolant temperature was 566 K (560 °F), and all the control rod and shutdown banks were withdrawn. The cycle operation calculation step was treated with

each data to the calendar days given by reference [3]. It should be noted that the days with zero core power (e.g., days 98 through 148 in cycle 1) were neglected.

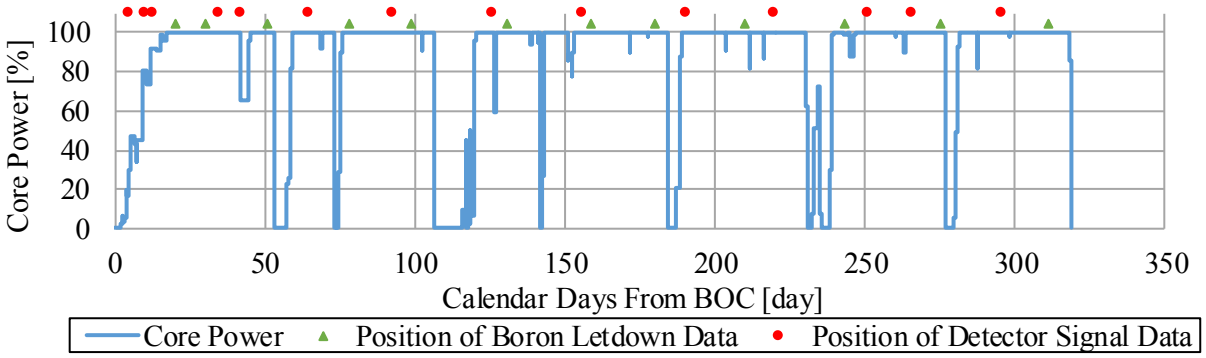

Figure 4. Cycle 2 Operation Diagram.

3. CALCULATION RESULTS

3.1. Cycle 1 Results

First, the HZP physics test calculation was performed. The calculation results of the CBC, CRBW, and ITC are summarized in Table II [3]. To estimate the ITC, two types of perturbation calculations, which were -5 K (-9 °F) perturbation of all temperatures at 566 K (560 °F) condition and 5 K (9 °F) perturbation at 561 K (551 °F) were performed, and then, the two ITCs were averaged [16].

Table II. HZP Physics Test Results of Cycle 1.

	Control Rod and Shutdown Bank Pattern	Meas. Data [3]	Calc. Result	
			JENDL-4.0	ENDF/B-VII.1
CBC [ppm]	All rods out (ARO)	975	956	956
	D in	902	896	897
	C, D in	810	799	800
	A, B, C, D in	686	665	665
	A, B, C, D, S_E, S_D, S_C in	508	477	477
CRBW [pcm]	D in	788	781	781
	C with D in	1203	1245	1249
	B with D, C in	1171	1202	1200
	A with D, C, B in	548	589	595
	S_E with D, C, B, A in	461	507	512
	S_D with D, C, B, A, S_E in	772	789	790
	S_C with D, C, B, A, S_E, S_D in	1099	1104	1103
ITC [pcm/°F]	ARO	-1.75	-2.14	-2.15
	D in	-2.75	-3.22	-3.23
	C, D in	-8.01	-7.74	-7.75

The calculation results of the CBC agreed well with the measurement data within approximately 30 ppm, which showed the same tendency as those appeared in previous studies. In terms of the CRBW, the calculation results also showed good agreement within approximately 50 pcm. The calculation results of

the ITC was different from the measurement data by approximately 0.4 pcm/°F. Moreover, the difference between the JENDL-4.0 and ENDF/B-VII.1 calculation results was small.

Then, the cycle operation calculation was performed. The calculation results of the boron letdown and radial/axial detector signals are shown in Figures 5 and 6. The measurement data of the boron letdown and detector signals were provided on 29 and 24 core exposure points, respectively. The calculation results of the radial/axial detector signals in Figure 6 are provided by the root mean square (RMS) of the difference between the measurement data and calculation results as:

$$RMS_{Radial} = \sqrt{\frac{\sum_{x,y}\left(\sum_z R(x,y,z)^{Meas.} - \sum_z R(x,y,z)^{Calc.}\right)^2}{N_{x,y}}}, \quad (1)$$

$$RMS_{Axial} = \sqrt{\frac{\sum_{z}\left(\sum_{x,y} R(x,y,z)^{Meas.} - \sum_{x,y} R(x,y,z)^{Calc.}\right)^2}{N_{z}}}, \quad (2)$$

where, RMS_{Radial} and RMS_{Axial} are the RMS of the differences between the measurement data and calculation results integrated over the radial and axial directions, respectively. $N_{x,y}$. and N_z are the numbers of the detector points for the radial (x and y) and axial (z) directions, respectively, and R is the detector signal.

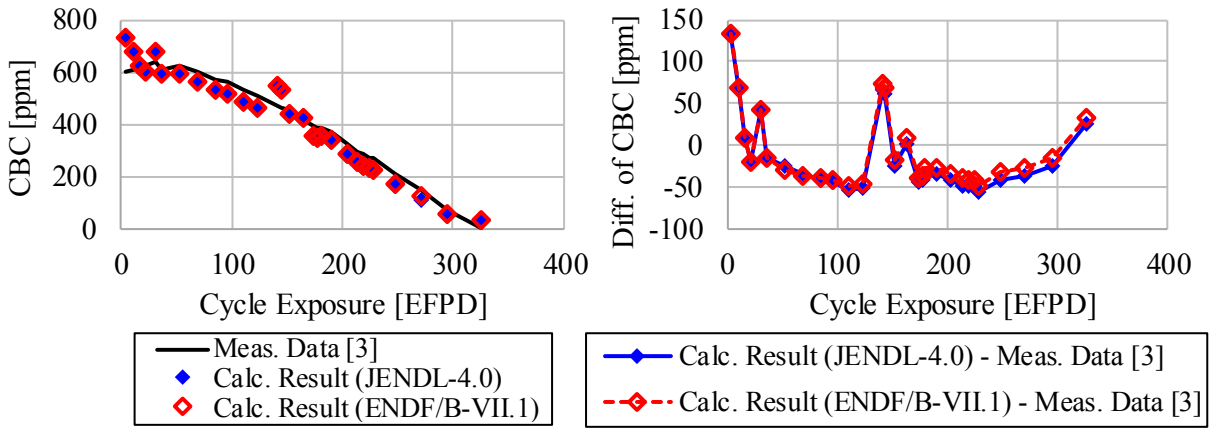

Figure 5. Boron Letdown Results of Cycle 1.

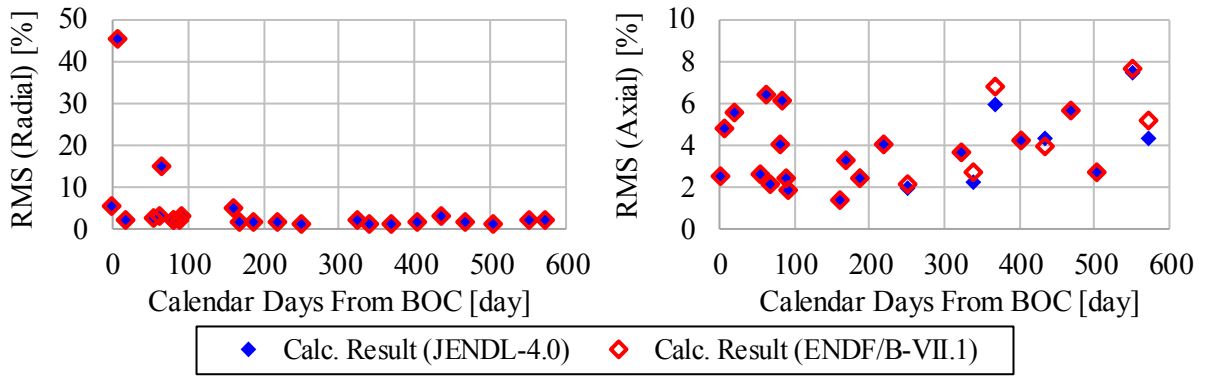

Figure 6. Detector Signal Results of Cycle 1 (Left: Radial, Right: Axial).

In terms of the boron letdown in Figure 5, most of the calculation results showed good agreement with the measurement data within approximately 50 ppm. For some calculation results, the differences from the measurement data was more than 50 ppm. The most plausible explanation for this large discrepancy is that the core power rapidly changed just before such measurement points and all the control rod and shutdown banks were assumed to be withdrawn (ARO approximation). The difference between the JENDL-4.0 and ENDF/B-VII.1 calculation results became large during the cycle operation and was approximately 10 ppm at the end of cycle (EOC). This tendency indicates that the difference between the JENDL-4.0 and ENDF/B-VII.1 calculation results would be due to the discrepancy of cross sections and inventories for some heavy nuclides such as Pu and Am and fission product nuclides. Thus, the investigation from the microscopic viewpoint will be necessary in future studies. From Figure 6, most of the calculation results of the radial detector signals also showed good agreement with the measurement data within approximately 5 % of the RMS difference. The RMS differences on the days 7 and 66 were as high as ~45 % and ~15%, respectively. The reason for these large discrepancies is that the core would be on a transient condition on these days as discussed in reference [10]. In terms of the axial detector signals, many calculation results showed large differences due to the discrepancy of axial offset (AO) caused by the ARO approximation during the cycle operation. The comparison between the JENDL-4.0 and ENDF/B-VII.1 calculation results showed that they were almost same at any cycle exposures.

3.2. Cycle 2 Results

First, the calculation results of the CBC, CRBW, and ITC on the HZP physics test calculation of cycle 2 are summarized in Table III [3].

Table III. HZP Physics Test Results of Cycle 2.

	Control Rod and Shutdown Bank Pattern	Meas. Data [3]	Calc. Result	
			JENDL-4.0	ENDF/B-VII.1
CBC [ppm]	ARO	1405	1361	1366
	C in	1273	1264	1268
CRBW [pcm]	D in	426	468	469
	C in	1014	1003	1011
	B in	716	728	719
	A in	420	394	404
	S_E in	438	423	429
	S_D in	305	353	350
	S_C in	307	353	350
	S_B in	781	801	800
	S_A in	326	372	366
ITC [pcm/°F]	ARO	-1.71	1.58	1.81

The calculation results of the CBC and CRBW agreed well with the measurement data within approximately 50 ppm. Compared with the cycle 1 results presented in Table II, the differences between the JENDL-4.0 and ENDF/B-VII.1 calculation results became slightly large, which would be due to the difference of spent fuel assembly condition (e.g., the exposure, actinide and fission product nuclide densities) at the cycle 1 EOC. On the other hand, the calculation results of the ITC showed an extremely large difference and these showed positive values. From the qualitative viewpoint, the ITC potentially became the positive value in the high boron concentration condition. Thus, the calculation results of the ITC became positive values because the boron concentration was approximately more than 1360 ppm. It is noted that the positive value of ITCs in the cycle 2 HZP physics test was also discussed in reference

[17] from the viewpoint of the inconsistent relationship between the ITC and the boron concentration. In future studies, further investigation will be necessary.

Then, the cycle operation calculation was performed. The calculation results of the boron letdown and radial/axial detector signals are shown in Figures 7 and 8. The measurement data of the boron letdown and detector signals were provided on 12 and 14 core exposure points, respectively.

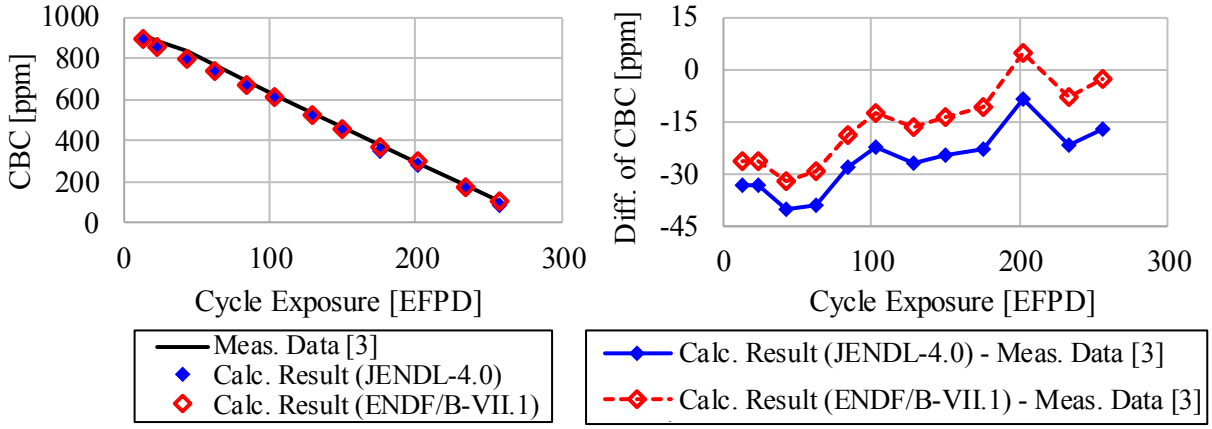

Figure 7. Boron Letdown Results of Cycle 2.

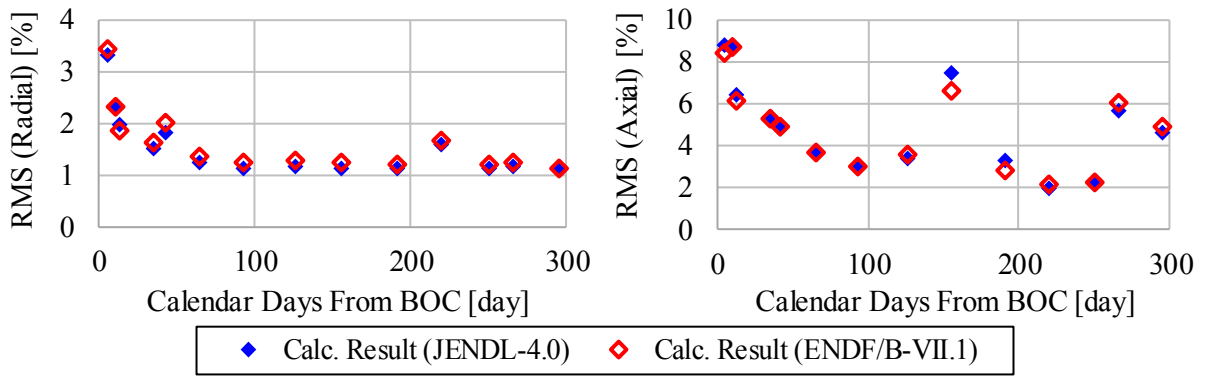

Figure 8. Detector Signal Results of Cycle 2 (Left: Radial, Right: Axial).

In terms of the boron letdown, the calculation results (Figure 7) agreed well with the measurement data within 45 ppm. Similar to the cycle 1 results shown in Figure 5, the difference between the JENDL-4.0 and ENDF/B-VII.1 calculation results became large from approximately 7 ppm at the BOC to approximately 15 ppm at the EOC. From Figure 8, the calculation results of the radial detector signals also showed good agreement with the measurement data within 4 % of the RMS difference. On the other hand, in terms of the axial detector signals, the RMS differences on some cycle exposure became large because of essentially the same reason as in cycle 1 (i.e., the ARO approximation). As with cycle 1, the JENDL-4.0 and ENDF/B-VII.1 calculation results were almost the same at any cycle exposures.

4. CONCLUSIONS

The BEAVRS benchmark was analyzed by the CASMO5/SIMULATE5 using the JENDL-4.0 and ENDF/B-VII.1. Through comparison of the calculation results with the measurement data, the validity of

the authors' calculation was analyzed. The study also focused on the influence of the nuclear data libraries used in the CASMO5/SIMULATE5.

The calculation results for the HZP physics test and cycle operation of cycles 1 and 2 showed good agreement with the measurement data, and the same tendency has been reported in previous studies. Thus, the authors' calculations using the CASMO5/SIMULATE5 well simulated the BEAVRS benchmark. In addition, the results of the JENDL-4.0- and ENDF/B-VII.1-based calculations were compared. Although approximately 15 ppm difference of boron letdown in the cycle operation was observed between them, no significant difference was seen for other core parameters (e.g., the radial/axial detector signals). Thus, the influence of the two nuclear data library was small on the present results.

REFERENCES

1. *CASMO5 User's Manual*, Studsvik Scandpower, Inc., SSP-07/431, (2012).
2. *SIMULATE5 User's Manual*, Studsvik Scandpower, Inc., SSP-10/438, (2012).
3. *MIT Benchmark for Evaluation And Validation of Reactor Simulations RELEASE rev. 2.0.2*, MIT Computational Reactor Physics Group, (2018).
4. V. Bykov et al., "Solution of the BEAVRS Benchmark Using CASMO-5 / SIMULATE-5 Code Sequence, "*Proc. PHYSOR2016*, Sun Valley, ID, May 1-5, 2016, (2016). [DVD-ROM].
5. B. S. Collins *et al.*, "Simulation of the BEAVRS Benchmark using VERA," *Proc. of M&C2017*, Jeju, Korea, Apr. 16-20, 2017, (2017). [USB].
6. H. Lee *et al.*, "Preliminary Simulation Results of BEAVRS Three-dimensional Cycle 1 Wholecore Depletion by UNIST Monte Carlo Code MCS," *Proc. of M&C2017*, Jeju, Korea, Apr. 16-20, 2017, (2017). [USB].
7. G. Gunow *et al.*, "Accuracy and Performance of 3D MOC for Full-Core PWR Problem," *Proc. of M&C2017*, Jeju, Korea, Apr. 16-20, 2017, (2017). [USB].
8. M. Suzuki *et al.*, "Analysis of BEAVRS Revision 2.0 LWR Whole Core Calculation Using MVP with JENDL-4.0," *Proc. of M&C2017*, Jeju, Korea, Apr. 16-20, 2017, (2017). [USB].
9. M. Zilly *et al.*, "Analyzing the BEAVRS HZP Case with KMACS Using 2-group Data from SCALE-NEWT, HELIOS and nTRANCER," *Proc. of M&C2017*, Jeju, Korea, Apr. 16-20, 2017, (2017). [USB].
10. D. O. Grady *et al.*, "Analysis of the BEAVRS Benchmark Using the TRITON/PARCS/PATHS Two-Step Sequence," *Proc. PHYSOR2018*, Cancun, Mexico, Apr. 22-26, 2018, (2018). [USB].
11. L. Liponi *et al.*, "Analysis of the MIT BEAVRS Benchmark Cycle 1 Using the DRAGON5/PARCS Code Sequence," *Proc. PHYSOR2018*, Cancun, Mexico, Apr. 22-26, 2018, (2018). [USB].
12. C. Wan *et al.*, "Uncertainty Analysis for the Core Simulation of Cycle 1 of the BEAVRS Benchmark Problem," *Proc. BEPU2018*, Lucca, Italy, May 13-19, 2018 (2018). [USB].
13. K. Shibata *et al.*, "JENDL-4.0: A New Library for Nuclear Science and Engineering," *J. Nucl. Sci. Technol.*. **48**(1), pp. 1-30, (2011).
14. M. B. Chadwick *et al.*, "ENDF/B-VII.1 nuclear data for science and technology: Cross sections, covariances, fission product yields and decay data," *Nucl. Data Sheets*, **112**(12), pp. 2887-2996, (2011).
15. J. Rhodes *et al.*, "CASMO5 JENDL-4.0 and ENDF/B-VII.1beta4 libraries," *Proc. of PHYSOR2012*, Knoxville, TN, Apr. 15-20, 2012, (2012). [CD-ROM].
16. B. Forget, *Integral Full Core Multi-Physics PWR Benchmark with Measured Data*, FY 2014 R&D Final Project Reports (NEUP Project 14-6742), Nuclear Energy University Program (NEUP), U. S. Department of Energy, (2018).
17. D. Kerdraon *et al.*, "ANDROMEDE calculations on BEAVRS benchmark (GABv2 / COCAGNE)," Proc. ICAPP2019, Juan-les-pins, France, May 12-15, 2019, (2019).